JOURNAL OF MAGNETIC RESONANCE IMAGING 33:1321–1329 (2011)

Original Research

Measurement of Aortic Arch Pulse Wave Velocity in Cardiovascular MR: Comparison of Transit Time Estimators and Description of a New Approach

Anas Dogui, PhD,[1*] Alban Redheuil, MD, PhD,[1–3] Muriel Lefort, BS,[1] Alain DeCesare, PhD,[1] Nadjia Kachenoura, PhD,[1] Alain Herment, PhD,[1] and Elie Mousseaux, MD, PhD[1–3]

Purpose: To investigate the efficiency of a new method (TT-Upslope) for transit time (Δt) estimation from cardiovascular MR (CMR) velocity curves.

Materials and Methods: Fifty healthy volunteers (40 ± 15 years) underwent applanation tonometry to estimate carotid–femoral pulse wave velocity (cf-PWV) and carotid pressure measurements, and CMR to estimate aortic arch-PWV and ascending aorta distensibility (AAD). The Δt was calculated with TT-Upslope by minimizing the area delimited by two sigmoid curves fitted to the systolic upslope of the ascending (AAC) and descending (DAC) aorta velocity curves, and compared with previously described methods: TT-Point using the half maximum of AAC and DAC, TT-Foot using AAC and DAC feet, and TT-Wave by minimizing the area between AAC and DAC curves using cross correlation.

Results: All the Δt methods provided a high reproducibility of arch-PWV. However, TT-Upslope and TT-Wave resulted in better correlations with aging ($r = 0.83/r = 0.83$ versus $r = 0.47/r = 0.72$), cf-PWV ($r = 0.69/r = 0.70$ versus $r = 0.34/r = 0.59$), and AAD ($r = 0.81/r = 0.71$ versus $r = 0.61/r = 0.60$). Furthermore, TT-Upslope resulted in stronger relationship between arch-PWV and AAD according to a theoretical model and provided better characterization of older subjects compared with TT-Wave.

Conclusion: Arch-PWV estimated with CMR using the TT-Upslope method was found to be reproducible and accurate, providing strong correlations with age and aortic stiffness indices.

Key Words: aortic stiffness; cardiovascular MR; pulse wave velocity; transit time
J. Magn. Reson. Imaging 2011;33:1321–1329.

AORTIC STIFFNESS IS recognized as a major risk factor in coronary heart disease (1,2), and is an independent predictor of cardiovascular mortality (3,4). Changes in aortic stiffness have high physiopathological relevance as these changes lead to an increase in aortic pulse pressure (5,6), and consequently cardiac pressure afterload, which promotes left ventricular hypertrophy (7). Aortic stiffness increases under the influence of several factors, the foremost being aging (8,9). Indeed, aging is a major factor of cardiovascular risk and is associated with a loss of elasticity of the aortic wall in adulthood even in healthy subjects (10–14).

The most clinically reliable index of aortic stiffness is pulse wave velocity (PWV) (15); the speed of propagation of the pressure or the velocity waves along the artery. The PWV is commonly calculated as the ratio between the distance separating two locations along the artery and the transit time needed for the pressure or velocity wave to cover this distance. Applanation tonometry is a well recognized technique for estimating pressure waveforms and arterial stiffness (15). However, concerning aortic stiffness, this technique can only provide an estimation of PWV along the whole carotid–femoral artery path. Furthermore, tonometry uses body surface measurements to approximate artery length and does not take into account the often torturous route of the vessels.

Cardiovascular MR (CMR) is increasingly used for measuring aortic arch PWV (arch-PWV) by using accurate aortic length and transit time between flow waves (16–25). If robust aortic length measurement is an obvious strength of CMR thanks to many three-dimensional (3D) imaging approaches available (26), transit time measurement remains a major challenge. Phase-contrast (PC) cine acquisitions provide an accurate assessment of flow waveforms within the ascending and the descending aorta, and may be used to estimate the transit time (Δt) between those two locations. Foot-to-foot methods are well established in tonometric studies for the transit time estimation between pressure waves (15) due to high temporal resolution and the avoidance of early reflected pressure waves. Transit time estimation using foot-to-foot

[1]Inserm U678/ UPMC Univ Paris 6, France.
[2]Radiology Department, APHP-European Hospital Georges Pompidou, Paris, France.
[3]Université Paris Descartes, Paris, France.
Contract grant sponsor: Xxxxxxx; Contract grant number: xxxxxxxx.
*Address reprint requests to: A. D., Laboratoire d'Imagerie Fonctionnelle, INSERM-U678/UPMC, 91 Boulevard de l'Hôpital, 75013, Paris, France. E-mail: anas.dogui@imed.jussieu.fr
Received October 26, 2010; Accepted February 14, 2011.
DOI 10.1002/jmri.22570
View this article online at wileyonlinelibrary.com.

measurements requires high temporal resolution to allow to accurately identifying the time of upstroke. PC acquisitions are currently hampered by low temporal resolutions relative to tonometric methods. Consequently, different methods have been previously described to estimate the transit time using CMR (16,18–25,27), but there is to date no fully standardized method for its determination.

Our primary goal in this study was to describe a new upslope-based method for Δt estimation using either flow or mean velocity curves extracted from the ascending and descending aorta, which was based on a previously described method (28). Our secondary goal was to compare this method with three previously described methods based on the commonly used foot-to-foot approaches, as well as the point-to-point and wave-to-wave approaches. The comparisons between methods were performed in terms of reproducibility, and correlation of arch-PWV with: (i) aging, (ii) carotid–femoral PWV (cf-PWV) estimated by tonometry, and (iii) local aortic distensibility estimated on the ascending aorta (AAD) from CMR and pulse pressure measurements.

MATERIALS AND METHODS

Fifty volunteers (age, 40 ± 15 years) were recruited in this study. None had any cardiovascular history, hypertension, or diabetes. All participants signed an informed consent approved by our local institutional ethic committee. All MR examinations were performed on a 1.5 Tesla (T) scanner (Signa LX; General Electric Medical Systems, Milwaukee, WI) using a cardiac phased-array coil and electrocardiography (ECG) -gated sequences.

To extract flow and mean velocity waves, PC sequences were acquired at the level of the bifurcation of the pulmonary trunk, perpendicular to both ascending and descending aorta. Hence, the ascending and descending aorta could be studied simultaneously. The PC data were acquired continuously using a retrospectively ECG-gated breathhold gradient echo sequence with a velocity encoding gradient in the through-plane direction, which provided phase-related pairs of modulus and velocity-encoded images. Retrospective gating was applied to avoid end diastolic gap in velocity data acquisition.

The scan parameters were as follows: repetition time = 8 ms (range, 7–9.5 ms), echo time = 3.5 ms (range, 2.8–4 ms), flip angle = 20°, matrix acquisition = 256 × 128 interpolated to 256 × 256, pixel size = 1.58 mm × 1.58 mm, slice thickness = 8 mm, views per segment = 2, encoding velocity = 200 cm/s, bandwidth = 31.3 KHz, and minimized ECG trigger delay = 10 ms. To minimize background offsets of velocity, the zero position of dataset was positioned at the middle of the cardiac coil corresponding to the middle of the sternum at the beginning of the acquisition. To further minimize background offsets and so that acquisition duration remained compatible with breath holding, a 50% rectangular field of view was used. Consequently, the two regions of interest for both the ascending and descending aorta were always close to the center of the acquired image and away from the PE-wraparound. View sharing was used resulting in an effective phase interval of 16 ms (range, 14–19 ms). The breathhold duration was fixed to 32 RR-intervals.

To estimate the 3D aortic length, axial and coronal sequences covering the whole aortic arch were acquired with a cine breathhold steady-state free-precession (SSFP) sequence using the following scan parameters: field-of-view = 370 mm × 370 mm, repetition time = 3.2 ms (range, 2.7–3.9 ms), echo time = 1.4 ms (range, 1.1–1.7 ms), flip angle = 50°, bandwidth = 125 KHz, slice thickness = 8 mm, pixel size = 1.65 mm × 1.92 mm, view per segment = 32, number of cardiac phases = 30, and phase interval = 33 ms (range, 21–50 ms).

To estimate AAD, axial cine SSFP images were acquired at the same level as the PC acquisition. For this specific SSFP acquisition: repetition time = 3.2 ms, echo time = 1.4 ms, view per segment = 12, and number of cardiac phases = 50. The phase interval ranged between 11 and 29 ms, depending on the heart rate.

Immediately after CMR acquisitions, applanation tonometry of both the right carotid artery and right femoral artery was performed with the Pulse Pen device (Diatecne, Milano, Italy) (29) to measure the carotid pulse pressure, and the carotid–femoral PWV (cf-PWV).

cf-PWV was defined as the distance traveled by the pulse wave divided by the transit time. The arterial distance was estimated by a tape ruler and defined as the difference between the suprasternal notch to femoral artery and the carotid to suprasternal notch distances. The transit time was measured between the feet of the pressure waveforms recorded at the carotid and femoral arteries.

The carotid pulse pressure was calculated after scaling tonometric measurements with the brachial mean and diastolic pressures (15) simultaneously recorded during the PC acquisitions using an oscillometric technique (Vital Signs Monitor, Welch Allyn Inc, Skaneateles Falls, NY). This approach permitted taking into account potential changes of the arterial condition of the subject due to his moving from the MR examination to the tonometric examination.

Image Analysis

Regional Aortic Arch Pulse Wave Velocity

The arch-PWV was calculated as the ratio between the 3D length of the aortic arch, and the transit time (Δt) between the velocity waveforms in the ascending and descending aorta. To estimate the 3D length of the aortic arch, the centers of the aortic lumen were first selected by an experienced user on each cine axial and coronal slices in a 3D Coordinate-System. Six to eight markers were defined for the ascending and the descending segment on axial slices, and three markers were defined for the top of the aortic arch on coronal slices. The 3D coordinates of the selected centers were computed from the DICOM headers of the

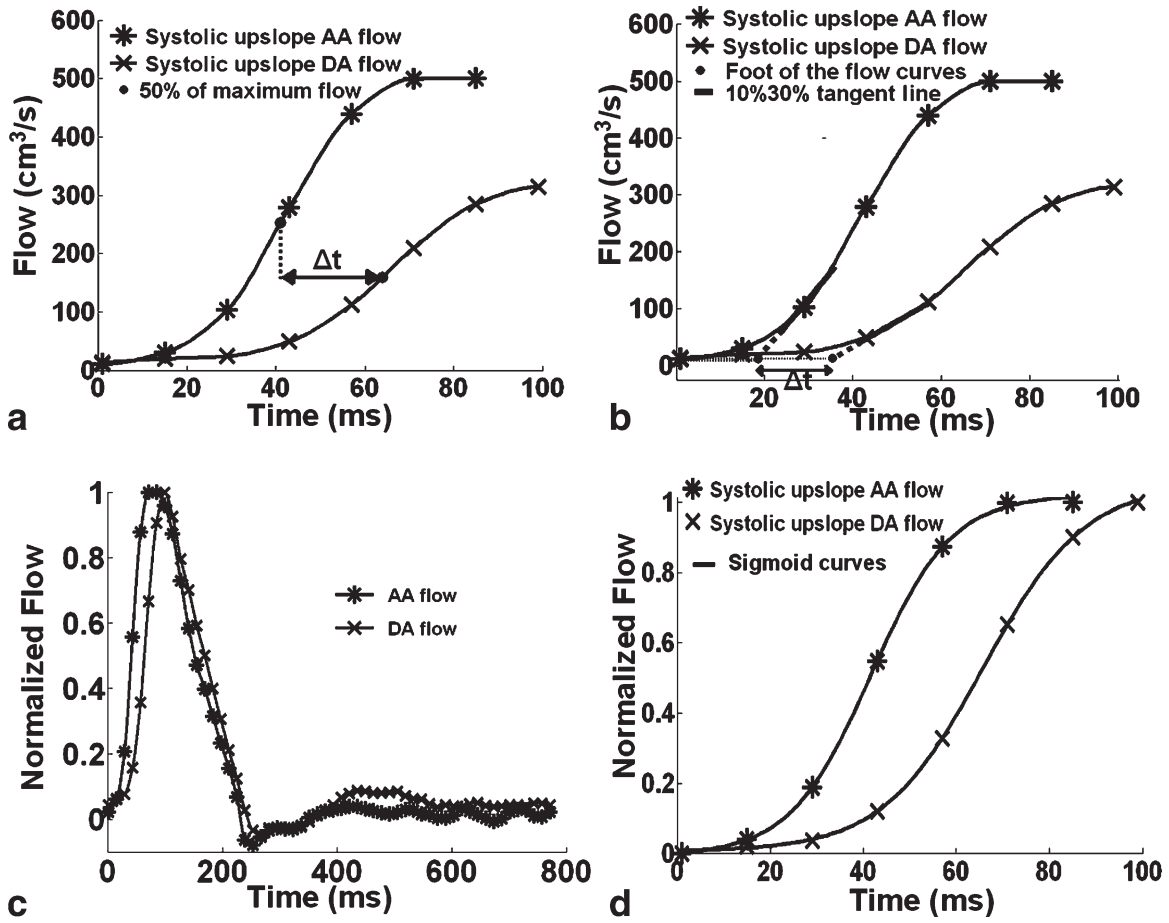

Figure 1. The four transit time (Δt) methods. **a**: TT-Point: Δt estimated from the point of 50% of maximum flow. **b**: TT-Foot: Δt estimated from the foot of the flow curves. **c**: TT-Wave: Δt estimated from the entire normalized flow curves using the cross correlation technique. **d**: TT-Upslope: Δt estimated analytically from the sigmoid curves fitted to the systolic upslope of both normalized flow curves.

MR images, and were interpolated with a 3D Bezier curve. The length of the 3D Bezier curve comprised between the ascending and descending aorta planes defined from the PC images was considered for the estimation of the arch-PWV. The estimation of this 3D aortic length was repeated by two independent operators.

To extract ascending and descending aorta flow and mean velocity curves, aortic lumen contours were semi-automatically detected from the modulus of the PC images using a robust segmentation technique based on a (2D + t) snake algorithm, as previously used (28) and validated (30). Contours were then superimposed on the velocity-encoded images. The aortic lumen contours of PC images were also estimated by two operators. Furthermore, to better characterize the initial portion of the flow and mean velocity curves, a systematic temporal shift of 3 phases was applied to the PC data acquisition before extracting the curves.

For each operator, the transit time (Δt) was calculated automatically from both flow and mean velocity curves using the TT-Upslope method, and three other methods previously used in MRI: TT-Point (17,18,25,31), TT-Foot (16,32), and TT-Wave (22,33).

TT-Point is a point-to-point method estimating Δt from the points where the velocity curves of the ascending and descending aorta reach their half maximum as shown in Figure 1a.

TT-Foot is a foot-to-foot method estimating Δt from the foot of the velocity curves of the ascending and descending aorta, based on the foot to foot technique most commonly used for the transit time estimation in tonometric studies (15). The foot of the curve was defined as the intersection between the horizontal line passing through the minimum point and the linear regression modeled between the initial 10% and 30% of the systolic upslope of the velocity curve as shown in Figure 1b.

TT-Wave is a wave-to-wave method estimating Δt from the entire velocity curves as shown in Figure 1c. It is based on the cross correlation technique, which applies a time-shift to the normalized velocity curves of the descending aorta until the highest correlation with the normalized velocity curves of the ascending aorta is obtained. The Δt was defined as the time shift providing the highest correlation between the two velocities.

TT-Upslope is an upslope-to-upslope method estimating Δt from the systolic up-slope of the velocity

curves and based on a previously described method (28). However, it differed from the latter on two features: (i) the Δt was estimated analytically using a sigmoid model instead of using temporal shifting of velocity curves with a predefined temporal step (1 ms), and (ii) the beginning of the systolic up-slope was defined using the maximum curvature of the velocity curves instead of its minimum.

First, the ascending portions between the first minimum and the maximum of the normalized velocity curves of both ascending and descending aorta were respectively fitted to sigmoid models Seg_A and Seg_D as shown in Figure 1d. The sigmoid model was defined as follows, and its parameters (a, b, x_0, dx) were automatically determined using the least squares minimization approach:

$$Seg(t) = b + \frac{a-b}{1+\exp(\frac{t-x_0}{dx})} t \in \Re. \quad [1]$$

Then, the transit time Δt was calculated as the time shift for which the area (Er) between the sigmoid models $Seg_A(t)/t \in [t_1, t_2]$ and $Seg_D(t)/t \in \Re$ is equal to zero. Here, t_1 and t_2 are the beginning and ending time of the systolic up-slope ascending aorta velocity curve. Therefore, the Δt was analytically determined as follows:

$$\Delta t = \Delta t_k \ with \ Er(\Delta t_k) = 0. \quad [2]$$

Where:

$$Er(\Delta t_k) = \int_{t_1}^{t_2} (Seg_A(t) - Seg_D(t - \Delta t_k))dt. \quad [3]$$

Here, Δt_k is a real ($\in \Re$). The systolic up-slope was defined as the portion of the velocity curves between the maximum upward curvature preceding the systolic peak and the peak velocity. Indeed, the velocity curves were interpolated with a time resolution of 1 ms to increase the number of points and were considered as parametric plane curves ($v_i = (x_u, y_i)$). The curvature ($Curv_i$) at each point i of coordinate (x_u, y_i) was then computed as follows (34):

$$Curv_i = \frac{4(y_{i+1} - 2y_i + y_{i-1})\Delta x_i - 4(x_{i+1} - 2x_i + x_{i-1})\Delta y_i}{((\Delta x_i)^2 + (\Delta y_i)^2)^{3/2}} \quad [4]$$

Here $\Delta x_i = \frac{1}{2}(x_{i+1} - x_{i-1})$, and $\Delta y_i = \frac{1}{2}(y_{i+1} - y_{i-1})$.

Local Ascending Aorta Distensibility

The local AAD was computed as follows:

$$AAD = \frac{S_s - S_d}{S_d \times \Delta P}. \quad [5]$$

Here, ΔP is the tonometric carotid pulse pressure; Ss and Sd are the maximal systolic and minimal diastolic areas of the aortic lumen at the level of the ascending aorta. These lumen areas were measured from SSFP cine MR acquisitions using the automatic segmentation technique as previously described (30).

Table 1
Subject Characteristics Expressed as Mean ± SD

Parameters	Subjects(n=50)
Age(years)	40±15
Body mass index ($kg.m^{-2}$)	23.73±3.52
Carotid systolic pressure (mmHg)	100.5±12.35
Carotid diastolic pressure (mmHg)	64.1±9.2
Carotid pulse pressure (mmHg)	35.7±10.5
AAD ($10^{-3}mmHg^{-1}$)	5.73±3.2
Aortic length (cm)	12.2±2.2
cf-PWV ($m.s^{-1}$)	7.19±3.17

AAD = local ascending aorta distensibility estimated from MRI aortic surfaces and carotid pulse pressures; cf-PWV = global aortic PWV assessed with tonometry.

Statistical Analysis

The results of arch-PWV were provided for all methods as mean ± standard deviation (SD) for all subjects. Values were compared across methods and type of velocity curves using respectively the analysis of variance (ANOVA) and the Student's paired t-test.

The arch-PWV estimated by each transit time method was compared with both age and carotid–femoral PWV (cf-PWV) using a linear regression analysis, and to local ascending aorta distensibility (AAD) using a power regression analysis ($y = \frac{a}{x^n}$). This latter comparison was performed to study the relationship between arch-PWV estimated by the four transit time methods and AAD according to the Bramwell-Hill equation ($Distensibility = \frac{1}{\rho \times PWV^2}$) (35), which is commonly used in clinical practice (15). The correlation coefficients (r) were provided for all regression analysis, and the statistical significance was indicated by $P < 0.05$ on all tests.

Aortic length and Δt in regard to all methods were measured by two independent operators using the same dataset. The inter-observer variability was studied using the mean difference, and the coefficient of variation (CV) defined as the mean of the absolute difference between the two series of measurements divided by the mean of both measurements.

RESULTS

The characteristics and estimated hemodynamic and aortic stiffness indices for the 50 volunteers are summarized in Table 1.

Arch-PWV

As summarized in Table 2, despite the facts that the mean arch-PWV estimated by TT-Upslope was lower than those estimated by TT-Wave, TT-Point, and TT-Foot, differences between arch-PWV values across Δt estimation methods did not reach significance according to the ANOVA test.

Table 2
Arch-PWV Estimated Using the Four Transit Time (Δt) Assessment Methods and From Both Flow and Mean Velocity Curves

Methods of Δt	Arch-PWV (m/s) (n=50) Using flow curves	Using mean velocity curves	*P*
TT-Wave	4.71±1.8	4.76±1.87	0.16
TT-Upslope	4.33±1.3	4.34±1.33	0.34
TT-Foot	4.73±1.82	4.59±1.68	0.43
TT-Point	4.73±1.47	4.86±1.61	0.02

Mean ± SD of arch-PWV are reported and compared across methods. No significant differences of arch-PWV were found across the Δt methods; *P* is the statistical value resulted from the comparison between arch-PWV values estimated from flow and mean velocity curves.

Arch-PWV values were not significantly different when using mean velocity curves instead of flow curves except for the TT-point method ($P = 0.02$).

Relationship of Arch-PWV to Age and Stiffness Indices

Arch-PWV estimated by the four Δt methods was compared with aging, as well as local aortic stiffness AAD and global aortic stiffness cf-PWV. Arch-PWV measured with the four Δt methods increased linearly with age as shown in Figure 2 and Table 3. However, the strongest linear relationships were found between wave-based methods (TT-Wave and TT-Upslope) compared with point-based methods (TT-Point and TT-foot). When considering all subjects the relationship with age of arch-PWV values measured from TT-upslope and TT-wave were not significantly different. However, when stratifying the study population according to age, the relationship of arch-PWV with aging was significant using both methods but remained significant only using TT-upslope ($P = 0.04$) but not using the TT-wave method ($P = 0.07$) in subjects over 50 years (n = 13).

Arch-PWV measured with the four Δt methods also increased linearly with cf-PWV as shown in Figure 3 and Table 3. The strongest relationships with cf-PWV were found with Wave-based methods (TT-Wave and TT-Upslope) compared with point-based methods (TT-Point and TT-foot). When considering all subjects the relationship with cf-PWV of arch-PWV values measured from TT-upslope and TT-wave were not significantly different. However, when stratifying the study population according to age, the relationship of arch-PWV with cf-PWV was significant using both methods but remained significant only using TT-upslope ($P = 0.04$) but not using the TT-wave method ($P = 0.08$) in subjects over 50 years (n = 13).

Furthermore, arch-PWV was expectedly inversely related to AAD according to the theoretical Bramwell-

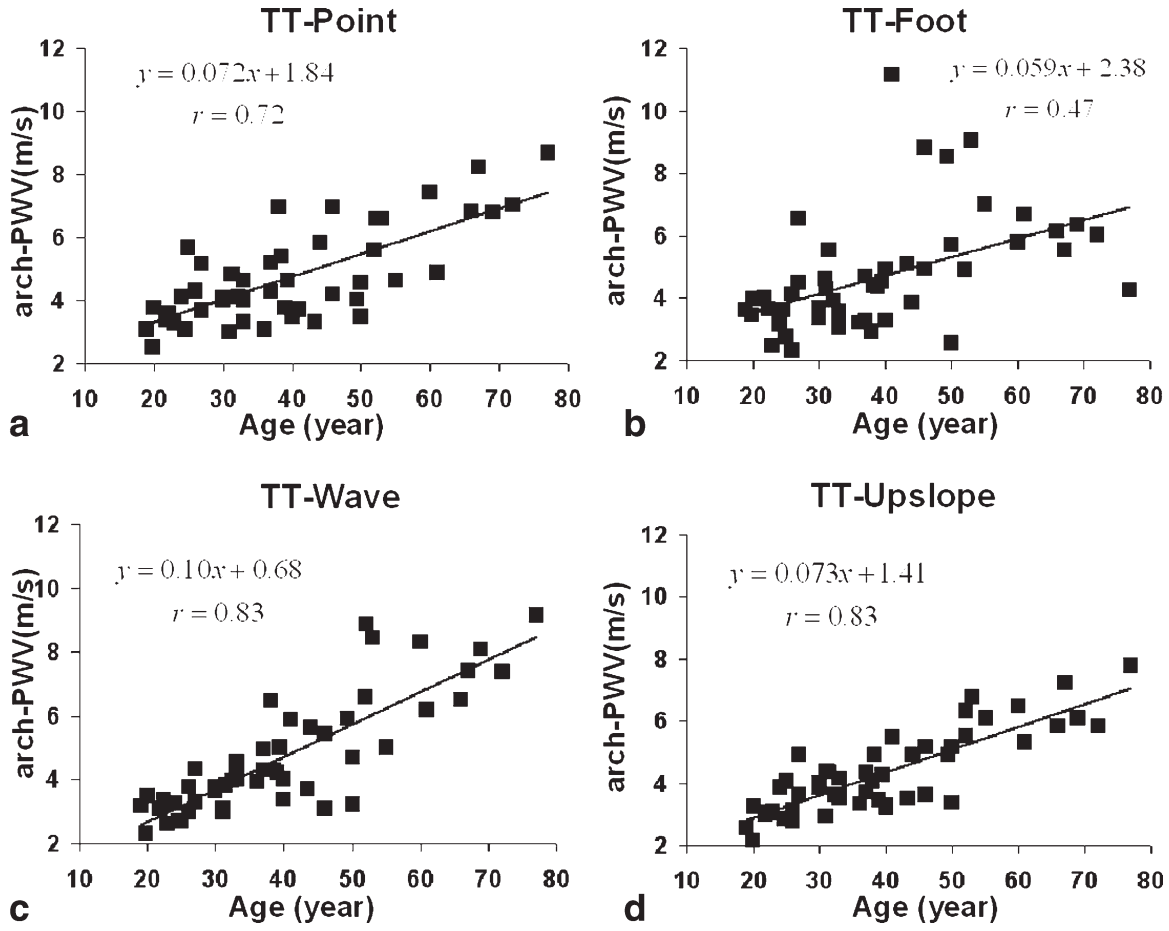

Figure 2. Variation of arch-PWV according to aging estimated by TT-Point (**a**), TT-Foot (**b**), TT-Wave (**c**), and TT-Upslope (**d**).

Table 3
Pearson Coefficients (r) of the Linear and Power Regressions Analysis Between Arch-PWV Estimated by the Four Transit Time (Δt) Methods and the Parameters of Age, cf-PWV, and AAD

	Using flow curves			Using mean velocity curves		
Methods of Δt	Age/arch-PWV	cf-PWV/arch-PWV	arch-PWV/AAD	Age/arch-PWV	cf-PWV/arch-PWV	arch-PWV/AAD
TT-Wave	0.83 ($P<0.001$)	0.70 ($P<0.001$)	0.71 ($P<0.001$)	0.81 ($P<0.001$)	0.69 ($P<0.001$)	0.70 ($P<0.001$)
TT-Upslope	0.83 ($P<0.001$)	0.69 ($P<0.001$)	0.81 ($P<0.001$)	0.79 ($P<0.001$)	0.64 ($P<0.001$)	0.73 ($P<0.001$)
TT-Foot	0.47 ($P<0.001$)	0.34 ($P=0.013$)	0.61 ($P<0.001$)	0.48 ($P<0.001$)	0.26 ($P=0.047$)	0.59 ($P<0.001$)
TT-Point	0.72 ($P<0.001$)	0.59 ($P<0.001$)	0.6 ($P<0.001$)	0.64 ($P<0.001$)	0.53 ($P<0.001$)	0.55 ($P<0.001$)

AAD = local ascending aorta distensibility estimated from MRI aortic surfaces and carotid pulse pressures; cf-PWV = global aortic PWV assessed with tonometry.

Hill model. Indeed, this relationship was well described with a power regression ($y = \frac{a}{x^n}$) as shown in Figure 4 and Table 3. The highest correlation between AAD and arch-PWV was found using the TT-Upslope method. The results of the power regression parameters (a,n) were, respectively, (3×10^{-4},1.4) using TT-Wave, (6×10^{-4},2.04) using TT-Upslope, (2×10^{-4},1.3) using TT-Foot, and (3×10^{-4},1.5) using TT-Point. These parameters were closer to those provided in theory by the Bramwell-Hill equation ($a = 1/\rho = 9 \times 10^{-4}$, $n = 2$), when the TT-Upslope method was used for the arch-PWV estimation.

As shown in Table 3, the correlation between arch-PWV, estimated from the different Δt methods, and age, cf-PWV as well as AAD were slightly better using flow curves instead of mean velocity curves except for the unchanged relationship with age concerning the TT-Foot method.

Reproducibility of Aortic Length, Δt, and Arch-PWV

The aforementioned inter-method comparisons and relationships of arch-PWV with age, cfPWV and AAD yielded similar results for the two operators. The inter-observer reproducibility of aortic length measurement by the 3D approach and Δt estimation by the four methods were high. Mean differences of the 3D aortic length estimated by two operators were 2 ± 5 mm, and the inter-observer variation coefficient was

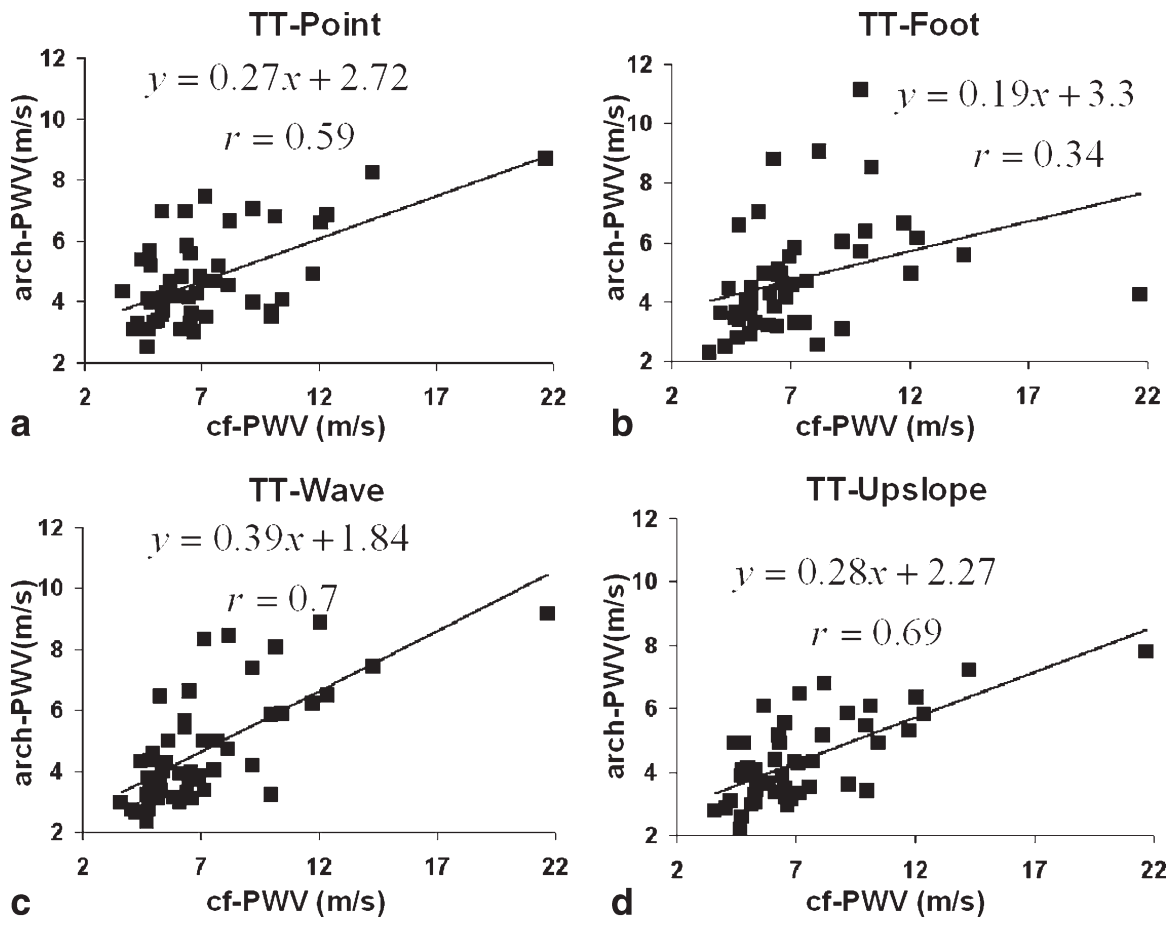

Figure 3. Variation of arch-PWV according to cf-PWV estimated by TT-Point (**a**), TT-Foot (**b**), TT-Wave (**c**), and TT-Upslope (**d**).

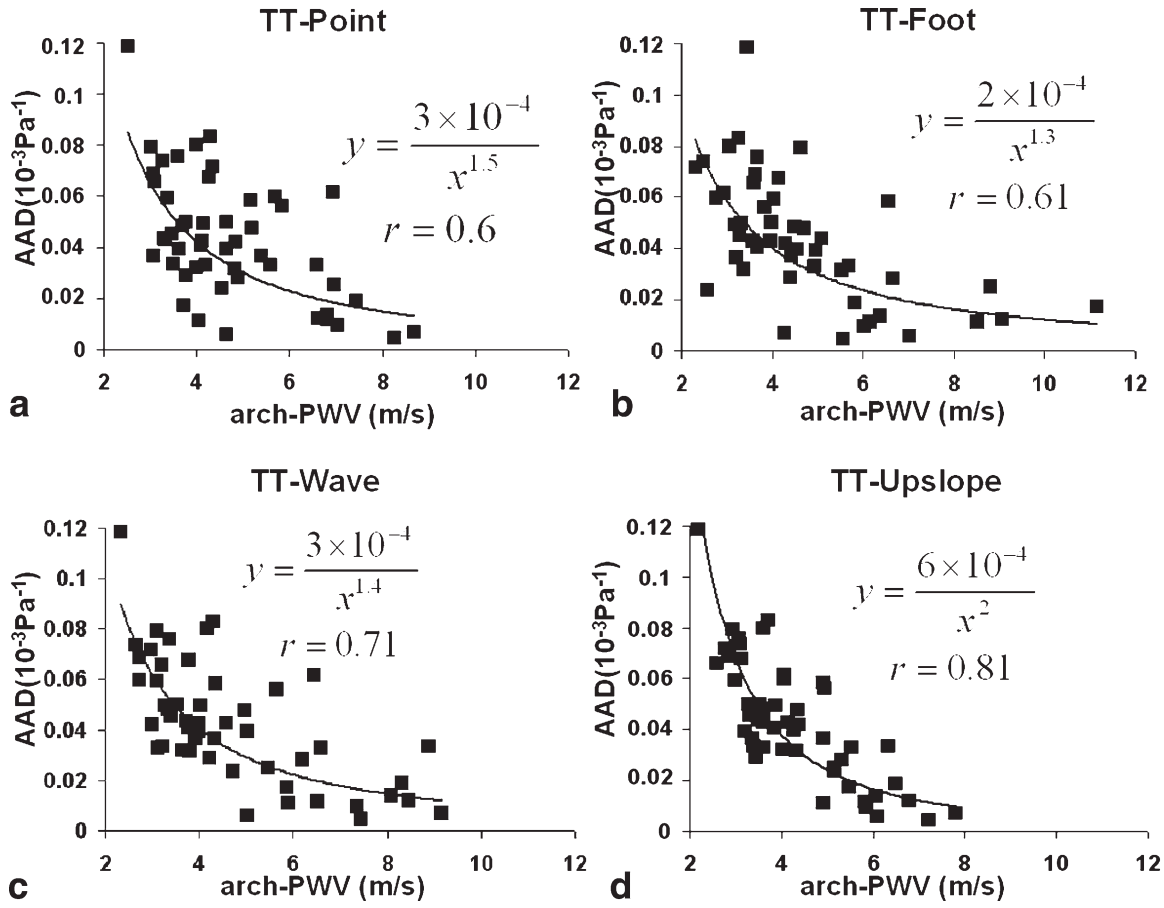

Figure 4. Variation of arch-PWV according to AAD estimated by TT-Point (**a**), TT-Foot (**b**), TT-Wave (**c**), and TT-Upslope (**d**).

4 ± 2%. Table 4 shows the inter-observer variation coefficients and mean differences of Δt and the resulting arch-PWV using the four estimation methods. The inter-observer variation coefficients were unchanged by using flow curves instead of mean velocity curves ($P > 0.05$).

DISCUSSION

The aim of this study was to describe a new Δt estimation method, TT-Upslope, used to calculate arch-PWV with MRI, and to compare it with three previously described methods (TT-Point, TT-Foot, TT-Wave), in terms of correlation with aging, cf-PWV, and local distensibility AAD as well as reproducibility. Our main finding was that the TT-Upslope and the TT-Wave methods resulted in a better correlation of arch-PWV with aging, cf-PWV, and AAD. However, the TT-Upslope method was found to be more sensitive to characterize aging and global aortic stiffness in older individuals (>50 years) compared with TT-Wave. In addition, TT-Upslope was shown to describe the relationship between arch-PWV and AAD according to the Bramwell-Hill equation better than the TT-Wave method.

Overall, arch-PWV values found in our study were consistent with those obtained in previous studies using CMR, when considering similar methods for Δt estimation (16,17,19–21,28). The studies in Mohiaddin et al (16) and Grotenhuis et al (19) used foot-to-foot methods. However, they differed in the determination of the foot of the systolic upslope of the velocity wave. In Mohiaddin et al (16) the foot was determined from the beginning of the systolic upslope of the velocity curves, as with the TT-Foot method, whereas in Grotenhuis et al (19), the foot of the curves was determined from the systolic upslope between 20% and 80% of the maximum velocity value. The mean value of arch-PWV was found in Mohiaddin et al (16) equal to 4.3 ± 0.7 m/s (age, 10–19 years; n = 16), whereas in Grotenhuis et al (19) the mean value of arch-PWV was 4.3 ± 0.5 m/s (age, 29 ± 8 years; n = 10). Another study Groenink et al (17) used the TT-Point method for the Δt estimation, and the arch-PWV was 3.8 ± 0.7 m/s (age, 28 ± 6 years; n = 26). A study by Lalande et al (21) presented a method for Δt estimation based on a least squares minimization considering the entire shape of the velocity curves, and reported a mean value of arch-PWV of 3.6 ± 0.64 m/s (age, 25 ± 5 years; n = 21). Furthermore, this wave-to-wave method is used in dedicated software (Giuseppe Lio, DiaTecne, Milan, Italy) (36). A recent study (28), used an upslope-to-upslope method, which estimated Δt by minimizing the area between systolic upslope portions of velocity curves by temporal shifts of 1 ms. This study reports for subjects between 30 and 50 years (n = 46) a mean value of arch-PWV equal to 4.75 ± 1.25 m/s.

Table 4
Mean Difference ± SD (MD) and Coefficient of Variation (CV) of Inter-observer Variability of Transit Time (Δt) and Arch-PWV Estimated With the Four Methods and From Flow Curves

Methods of Δt	MD of Δt (ms)	CV of Δt (%)	MD of arch-PWV (m/s)	CV of arch-PWV (%)
TT-Wave	0.08±1.8	4±7	0.12±0.58	6±7
TT-Upslope	0.2±2.0	4±5	0.05±0.35	6±5
TT-Foot	0.7±1.7	5±5	0.04±0.41	6±4
TT-Point	0.2±2.7	5±8	0.13±0.66	7±8

TT-Upslope and TT-Wave methods provided the best correlations between arch-PWV and aging, cf-PWV, and AAD. However, the arch-PWV assessed with TT-Upslope was better related to AAD according to the Bramwell-Hill equation. Furthermore, TT-Upslope yielded arch-PWV values more strongly related to aging and cf-PWV compared with TT-Wave in subjects over 50 years of age. These findings suggest that restricting the wave analysis to the upslope alleviates the influence of the morphology of the downslope, which may be altered by aortic stiffening and disorganization of the flow during endsystole. Consequently, the upslope may be preferred to the entire flow curve to estimate Δt because of the unidirectional and reflectionless nature of the upslope of the velocity curve (20,37). Contrary to flow curves, TT-foot methods are preferred in the case of pressure curves estimated by tonometry due to early reflected pressure in case of high aortic stiffness.

Of note, the TT-Upslope used a sigmoid model, and thus the Δt was analytically calculated. This approach provided a more precise estimation of Δt than by using temporal shifting of velocity curves with a predefined temporal step (1 ms) as described in previous methods (28). Furthermore, the very initial systolic portion of the flow curve, preceding the true upstroke point is often characterized by significant fluctuation. Therefore, the true upstroke point can easily be mistaken using the minimum criterion which was used by the previous method (28). Therefore, the curvature approach used by the TT-Upslope method provided a better characterization of the very beginning of the systolic upslope on the velocity curve.

The TT-Upslope and TT-Wave were based on the analysis of more samples of the velocity curves than with the point-based method: TT-Foot and TT-Point. We can assume that curve-based methods are less sensitive to the trend of velocity curves extracted from PC data, and to its signal-to-noise ratio because it avoids the restriction of the analysis to only a few characteristic points of the velocity curves. Indeed, small changes in the morphology of the velocity curve during systole may be observed between ascending and descending aorta due to the descent of the aortic valve during early systole and due to different interactions between each segment of the aorta and the flow impulse during LV contraction. Thus, the velocity curve during systole may have a physiological widening and a decreasing upslope along the course of the aorta resulting in an artificial prolongation of the Δt. This effect is minimized by normalizing the two velocity curves by the maximal velocity before using the TT-Upslope and TT-Wave methods to estimate Δt. In addition, the low temporal resolution of PC data can hamper the determination of the foot and half maximum of the velocity curves. These issues could explain that the Δt estimation by two operators introduced a slightly less variability with TT-Upslope and TT-Wave than with TT-Foot and TT-Point methods.

In our study, a 3D approach was used to assess the aortic arch length from both the coronal and axial slices, rather than the 2D measurement which is usually performed from a single sagittal oblique section by a manual tracing of the centerline of the aorta (16–18,20). The advantage of a 3D technique is its ability to better take into account the 3D geometry of the aorta. Indeed, the curvature of the aortic arch is not always aligned in a specific plane regarding to the position of the ascending and descending aorta. We found a very low inter-observer variability using 3D centerline determination.

The inter-observer reproducibility of arch-PWV, introduced by the combination of the inter-observer reproducibility of both Δt and 3D aortic length measurements, was similar throughout the different Δt methods. Of note, the inter-observer variability of the arch-PWV was mainly due to the variability of Δt estimation than to the aortic length estimation. Indeed, the inter-observer variability of the first parameter was between 4% ± 5% and 5% ± 8% depending on the Δt methods, whereas the inter-observer variability of the second parameter was 4% ± 2%. Practically in CMR, both flow or mean velocity curves can be used to measure Δt. Overall, we found that using flow curves provided arch-PWV values with slightly higher correlation to age, cf-PWV, and AAD.

The main limitations in our study concern the relatively small number of subjects with very high aortic stiffness, and the necessity of invasive measurements to obtain reference values for arch-PWV which could be used for comparisons between the four Δt methods. However, in the present proof of concept study, the physiological criterion of age, and the use of largely validated aortic stiffness indices cf-PWV and AAD provided a significant separation between the different methods of Δt when the arch-PWV was estimated on 50 volunteers. Furthermore, comparing the different Δt methods by studying the relationship between arch-PWV and AAD according to a theoretical model is a new approach that was proposed in the present study. Comparisons between Δt methods could be further evaluated in the future in a patient population with highly altered aortic transit time intervals. In addition, the influence of the repetition time of the PC acquisition and subsequently its

temporal resolution in the PWV estimation with the different Δt methods could also be evaluated.

In conclusion, arch-PWV index was assessed noninvasively using four different transit time methods and from either flow or mean velocity curves. The arch-PWV estimated from flow curves and with both estimators TT-Upslope and TT-Wave resulted in a better correlation with aging, tonometric carotid–femoral PWV, as well as the local ascending aorta distensibility. Indeed, the TT-Upslope and TT-Wave methods could minimize the variability of foot-to-foot and point-to-point measurements inherent to low temporal resolution, signal-to-noise ratio, and varying profile of the velocity curves. However, the TT-Upslope method was found to be more sensitive to characterize aging and global aortic stiffness in older individuals (>50 years), and resulted in a better relationship between arch-PWV and aortic distensibility according to the Bramwell-Hill equation. Physicians need to be aware that aortic PWV estimated using CMR can vary between laboratories because different methodologies can be used.

REFERENCES

1. Franklin SS, Khan SA, Wong ND, Larson MG, Levy D. Is pulse pressure useful in predicting risk for coronary heart Disease? The Framingham heart study. Circulation 1999;100:354–360.
2. Ohtsuka S, Kakihana M, Watanabe H, Sugishita Y. Chronically decreased aortic distensibility causes deterioration of coronary perfusion during increased left ventricular contraction. J Am Coll Cardiol 1994;24:1406–1414.
3. Boutouyrie P, Tropeano AI, Asmar R, et al. Aortic stiffness is an independent predictor of primary coronary events in hypertensive patients: a longitudinal study. Hypertension 2002;39:10–15.
4. Laurent S, Boutouyrie P, Asmar R, et al. Aortic stiffness is an independent predictor of all-cause and cardiovascular mortality in hypertensive patients. Hypertension 2001;37:1236–1241.
5. Benetos A. Pulse pressure and cardiovascular risk. J Hypertens Suppl 1999;17:S21–S24.
6. Nichols WW, Edwards DG. Arterial elastance and wave reflection augmentation of systolic blood pressure: deleterious effects and implications for therapy. J Cardiovasc Pharmacol Ther 2001;6: 5–21.
7. Nussbacher A, Gerstenblith G, O'Connor FC, et al. Hemodynamic effects of unloading the old heart. Am J Physiol 1999;277(Pt 2): H1863–H1871.
8. Benetos A. [Accelerators of arterial aging]. Rev Med Interne 2006; 27(Suppl 2):S44–S45.
9. Giannattasio C. Pathophysiology of central blood pressure and arterial stiffness. Central aortic blood pressure: Les Lab Servier 2008;49–53.
10. Avolio AP, Chen SG, Wang RP, Zhang CL, Li MF, O'Rourke MF. Effects of aging on changing arterial compliance and left ventricular load in a northern Chinese urban community. Circulation 1983;68:50–58.
11. Benetos A, Laurent S, Hoeks AP, Boutouyrie P, Safar ME. Arterial alterations with aging and high blood pressure. A noninvasive study of carotid and femoral arteries. Arterioscler Thromb Vasc Biol 1993;13:90–97.
12. Rerkpattanapipat P, Hundley WG, Link KM, et al. Relation of aortic distensibility determined by magnetic resonance imaging in patients > or =60 years of age to systolic heart failure and exercise capacity. Am J Cardiol 2002;90:1221–1225.
13. Mohiaddin RH, Underwood SR, Bogren HG, et al. Regional aortic compliance studied by magnetic resonance imaging: the effects of age, training, and coronary artery disease. Br Heart J 1989;62: 90–96.
14. McEniery CM, Yasmin, Hall IR, Qasem A, Wilkinson IB, Cockcroft JR. Normal vascular aging: differential effects on wave reflection and aortic pulse wave velocity: the Anglo-Cardiff Collaborative Trial (ACCT). J Am Coll Cardiol 2005;46:1753–1760.
15. Laurent S, Cockcroft J, Van Bortel L, et al. Expert consensus document on arterial stiffness: methodological issues and clinical applications. Eur Heart J 2006;27:2588–2605.
16. Mohiaddin RH, Firmin DN, Longmore DB. Age-related changes of human aortic flow wave velocity measured noninvasively by magnetic resonance imaging. J Appl Physiol 1993;74:492–497.
17. Groenink M, de Roos A, Mulder BJ, et al. Biophysical properties of the normal-sized aorta in patients with Marfan syndrome: evaluation with MR flow mapping. Radiology 2001;219:535–540.
18. Groenink M, de Roos A, Mulder BJ, Spaan JA, van der Wall EE. Changes in aortic distensibility and pulse wave velocity assessed with magnetic resonance imaging following beta-blocker therapy in the Marfan syndrome. Am J Cardiol 1998;82:203–208.
19. Grotenhuis HB, Westenberg JJ, Steendijk P, et al. Validation and reproducibility of aortic pulse wave velocity as assessed with velocity-encoded MRI. J Magn Reson Imaging 2009;30:521–526.
20. Vulliemoz S, Stergiopulos N, Meuli R. Estimation of local aortic elastic properties with MRI. Magn Reson Med 2002;47:649–654.
21. Lalande A, Khau Van Kien P, Walker PM, et al. Compliance and pulse wave velocity assessed by MRI detect early aortic impairment in young patients with mutation of the smooth muscle myosin heavy chain. J Magn Reson Imaging 2008;28:1180–1187.
22. Fielden SW, Fornwalt BK, Jerosch-Herold M, Eisner RL, Stillman AE, Oshinski JN. A new method for the determination of aortic pulse wave velocity using cross-correlation on 2D PCMR velocity data. J Magn Reson Imaging 2008;27:1382–1387.
23. Boonyasirinant T, Rajiah P, Setser RM, et al. Aortic stiffness is increased in hypertrophic cardiomyopathy with myocardial fibrosis: novel insights in vascular function from magnetic resonance imaging. J Am Coll Cardiol 2009;54:255–262.
24. Gang G, Mark P, Cockshott P, et al. Measurement of pulse wave velocity using magnetic resonance imaging. Conf Proc IEEE Eng Med Biol Soc 2004;5:3684–3687.
25. Zhao X, Pratt R, Wansapura J. Quantification of aortic compliance in mice using radial phase contrast MRI. J Magn Reson Imaging 2009;30:286–291.
26. Sugawara J, Hayashi K, Yokoi T, Tanaka H. Age-associated elongation of the ascending aorta in adults. JACC Cardiovasc Imaging 2008;1:739–748.
27. Rogers WJ, Hu YL, Coast D, et al. Age-associated changes in regional aortic pulse wave velocity. J Am Coll Cardiol 2001;38: 1123–1129.
28. Redheuil A, Yu WC, Wu CO, et al. Reduced ascending aortic strain and distensibility: earliest manifestations of vascular aging in humans. Hypertension 2010;55:319–326.
29. Salvi P, Lio G, Labat C, Ricci E, Pannier B, Benetos A. Validation of a new non-invasive portable tonometer for determining arterial pressure wave and pulse wave velocity: the PulsePen device. J Hypertens 2004;22:2285–2293.
30. Herment A, Kachenoura N, Lefort M, et al. Automated segmentation of the aorta from phase contrast MR images: validation against expert tracing in healthy volunteers and in patients with a dilated aorta. J Magn Reson Imaging 2010;31:881–888.
31. Kraft KA, Itskovich VV, Fei DY. Rapid measurement of aortic wave velocity: in vivo evaluation. Magn Reson Med 2001;46:95–102.
32. Stevanov M, Baruthio J, Gounot D, Grucker D. In vitro validation of MR measurements of arterial pulse-wave velocity in the presence of reflected waves. J Magn Reson Imaging 2001;14:120–127.
33. ElSayed HI, Kevin RJ, Alan BM, Jean MS, Richard DW. Measuring aortic pulse wave velocity using high-field cardiovascular magnetic resonance: comparison of techniques. J Cardiovasc Magn Reson 2010;12:26.
34. Frenkel M, Basri R. Curve matching using the fast matching method. Energy Minimizing Methods in Comput Vis Pattern Recognit 2003;2683.
35. Bramwell JC, Hill AV. The velocity of the pulse wave in man. Proc R Soc Lond B 1922;93:298–306.
36. Joly L, Perret-Guillaume C, Kearney-Schwartz A, et al. Pulse wave velocity assessment by external noninvasive devices and phase-contrast magnetic resonance imaging in the obese. Hypertension 2009;54:421–426.
37. Nichols WW, O'Rourke M. McDonald's blood flow in arteries. Theoretical, experimental and clinical principles. New York: Oxford Press; 1998.